Sustainable Food Technology

ROYAL SOCIETY OF CHEMISTRY

PAPER

View Article Online
View Journal

Cite this: DOI: 10.1039/d5fb00763a

Effects of quinoa flour addition on composite gluten-free bread: a comprehensive study of microstructural, oscillatory rheology and baking properties of bread dough

Priyana Garg,[ab] Gargi Ghoshal *[a] and Meenakshi Goyal[a]

The goal of this research was to conduct a microstructural study of gluten-free bread dough by incorporating nutrient rich quinoa flour (QF). Three levels of QF (40%, 50% and 60%) were used to prepare dough composites by replacing the dry blend of rice and maize flour (at a 1 : 1 ratio) while maintaining a hydration level of 90%, based on a 100 g flour basis. Fundamental rheological experiments were performed to access the viscoelastic behaviour of dough. The results indicated that quinoa addition modified the dough behaviour, evidenced by an increment in levels of G' and G'' from 4.629 Pa and 3.870 Pa to 4.880 Pa and 4.333 Pa, respectively, and early onset of gelatinisation revealed in the temperature sweep experiment (+7.8 °C) due to changes in starch–protein interactions with water. This study employed a power law model to evaluate its applicability to the rheological data of dough composites across various concentrations. DSC baked dough samples revealed a reduction in ΔH_G from 2.88 J g^{-1} to 1.85 J g^{-1} and ΔH_R from 5.21 J g^{-1} to 2.62 J g^{-1}, which correlated well with XRD analysis as RC values increased from 23.28% to 34.68%. Furthermore, an increment in short-range orderliness (*i.e.* DO and DD values from 1.06 to 1.25 and 1.06 to 1.38, respectively) indicated establishment of a stable structure and well-organized structure. After breadmaking, specific volume and cell density improved significantly which further coincided with the sensory analysis results. To sum up, the composite dough that included 50% QF displayed optimal rheological characteristics and baking quality in any instance. The results of the present study would provide necessary guidance for further improvements in making breads using gluten-free multi grain flours.

Received 28th October 2025
Accepted 24th February 2026

DOI: 10.1039/d5fb00763a

rsc.li/susfoodtech

Sustainability spotlight

The increasing consumer desire for nutritious food encourages the use of underutilized grains, such as quinoa, which necessitate fewer resources, enhance agricultural biodiversity and diminish reliance on conventional grains and animal-based products. Quinoa is nutrient-dense, climate-resilient grain that is essential to the world's food and nutrition security, but its extensive use is constrained by processing challenges. This research investigates sustainable food technology by utilizing quinoa as an alternative to traditional grain flour to produce gluten-free bread. The analysis of dough performance for gluten-free bread production fosters sustainable food diversity and bolsters resilient food systems. This corresponds with UN Sustainable Development Goals (SDG 2: zero hunger, SDG 3: good health and well-being, and SDG 12: responsible consumption and production).

1. Introduction

The food industry continually strives to develop new products without gluten in order to expand options for those with coeliac disease. The exclusion of gluten from bread often yields a liquid batter instead of dough, resulting in crumbly, unattractive bread. Gluten-free bread recipes mostly include refined flours combined with starches derived from sources other than wheat, including potato, maize, and cassava. According to Yazar *et al.*,[1] gluten-free breads vary greatly in nutritional composition, since they are often categorised as starch-based products having high fat and low protein content. The fortification of gluten-free breads with nutrient-dense ingredients demonstrates established physiological benefits for the celiac population and several associated conditions, including diabetes and hyperglycaemia.[2] Quinoa (*Chenopodium quinoa* Willd.) offers a naturally gluten-free flour that remains underutilized, serving as an exceptional source of macro- and microelements and containing bioactive compounds, including polyphenols.[3]

Researchers in the past had made attempts to produce gluten-free bread-like products utilising QF. Azizi *et al.*[3] used QF in conjunction with enzymes to enhance the volume and durability

[a]*Dr. S. S. B. University Institute of Chemical Engineering and Technology, Panjab University, Chandigarh, India. E-mail: gargighoshal@yahoo.co.in*
[b]*Amity School of Health Science, Amity University Punjab, Mohali, India*

of gluten-free bread. Sciarini *et al.*[2] studied the impact of different fractions and particle size of QF on rice-based gluten-free bread. Nevertheless, these studies mostly focused on the sensory and functional attributes of bread. The production of dough is an essential step in bread-making, as the characteristics of the dough profoundly influence the attributes of the final product. Gluten-free doughs exhibit reduced cohesion and elasticity relative to wheat dough. The dough intended for the production of biologically leavened bread must possess the strength to expand without breaking in response to the expansion of gas during baking. The capacity of gas retention and proofing tolerance in both conventional and gluten-free dough is contingent upon their structural-rheological characteristics.[4]

Also, mathematical modelling is essential in food processing operations to attain a sustainable processing sector.[5] To examine the structural alterations occurring in various dough systems during baking, the linear viscoelastic characteristics should be analysed using non-isothermal heating protocols (temperature sweep). Therefore, it would be intriguing to investigate the effects of non-isothermal heating on the rheological properties of gluten-free bread dough. Employing dynamic oscillatory measurement techniques inside the linear viscoelastic domain might yield a more thorough comprehension of gelatinisation kinetics. The rheological features of gluten containing dough structures are well-documented, but there is a dearth of publications relating the rheological and microstructural properties of quinoa-based dough with bread-making properties. Research into the ways in which the properties of the ingredients affect the structure of dough is becoming more necessary as a consequence of this. Hence, gluten-free breads were prepared utilising QF as a major ingredient at three different levels (40%, 50% and 60%) with a constant level of hydration (90%) based on a 100 g flour basis.

2. Materials and methods

2.1 Materials

Quinoa seeds were obtained from the National Bureau of Plant Genetic Resources (NBPGR), Shimla, India with accession no. EC507747 and cultivated at the local farm near Panjab University, Chandigarh, India. Then, they were processed utilising a laboratory-scale ball mill resulting in an extremely fine powder with particle sizes below 0.5 mm. The resulting quinoa powder constituted 10.56% moisture, 12.52% protein, 6.12% fat, and 2.53% ash on a dry basis. Other ingredients used for making dough composites including rice flour (11.02% moisture, 6.98% protein, and 0.78% fat and 1.22% ash, dry basis), corn flour (11.36% moisture, 6.24% protein, 4.1% fat, and 0.65% ash, dry basis), sugar, salt, yeast (Weissmill, instant active dry yeast), xanthan gum and hydrogenated vegetable oil were sourced from the local supermarket store.

2.2 Dough preparation and bread making

A gluten-free bread recipe without QF utilising maize and rice flour in equal proportions (1 : 1 ratio) served as the control. Other ingredients used to make the bread dough included xanthan gum (0.5 g), salt (1.5 g), sugar (4 g), dry yeast (5.5 g), and vegetable oil (8 g) as per 100 g of flour. In order to properly bake gluten-free breads, the water level was maintained at 90% throughout the bread-making process.[6] QF was added at three substitution levels (40%, 50%, and 60% of the total flour mixture of rice and maize flour) to prepare the dough samples. The relation of rice to maize flour in all dough preparations was maintained at 1 : 1. Following the initial step of combining all of the dry components, the next step was to incorporate yeast that had been previously dissolved in warm water (32 °C) and vegetable oil directly into the mixture. In order to produce the dough, all of the components were mixed together using an automated spiral dough hook mixer (SPAR Food Machinery Mfg. Co. Ltd., Taichung Hsien, Taiwan) for a duration of 2 min at a medium speed. Following this, the dough was kept aside for 45 min in a warm place to attain the required consistency and promptly folded in plastic wrap for rheological and microstructural analysis. For breadmaking, dough after acquiring the required consistency was further covered with damp cloth and kept in a proofing chamber (Continental, Ambala, India) in a greased pan ($L \times B \times H$: 22 × 11 × 5) for 60 min at 35 °C and 85% relative humidity. For baking, dough was kept in the conventional oven (Continental, India) at 175 °C for 45 min. After taking out the bread loaf from the pan, it was cooled at room temperature for 60 min and subsequently analysed.

2.3 Physiochemical analysis of flour blends and breads

The chemical composition of raw materials (*i.e.* quinoa, rice and corn flour) and flour mixtures used in this study was determined using the procedures detailed in AACC (2010)[7] including moisture content (44-01), protein (46-16, $N \times 6.25$), dietary fibre (32-05), fat (30-25) and ash (08-12). Carbohydrates were calculated by the difference method. AACC procedure no. 56-11 was used in order to determine the water and oil absorption capabilities of the flour mixtures. Weight and height of the bread loaf were noted down and the specific volume of the bread was calculated using the rapeseed displacement method of AOAC, 2006 (method no. 912.05).[8]

2.4 Oscillatory measurements of dough

A dynamic rheometer-MCR 102 (Anton Paar, Austria) was used to carry out the rheological assessments at a temperature of 25 °C, utilising a parallel plate geometry equipped with a solvent trap mechanism that had a gap of 2 mm and a diameter of 25 mm. For the purpose of rheological testing, dough samples were produced in a manner that was analogous to that of breadmaking, although yeast was not included in the formulation. Before initiating the experiment, samples were given time to rest for 5 min after being placed between the plates, in order to remove any residual tensions. First, the linear viscoelastic region (LVR) of samples was measured using amplitude sweep tests that encompassed a strain range extended from 0.001% to 100% at a constant frequency of 1 Hz. Following that, frequency sweep studies were conducted at a strain value of 0.5%, which was an outcome that was obtained from the amplitude sweep study. Furthermore, a temperature sweep

study was carried out at a frequency of 1 Hz and a strain value of 0.5% at temperatures that varied between 20 and 100 °C. The heating rate was maintained at 2 °C min^{-1}, comparable to the findings given by Ghoshal and Negi *et al.*[5] Data for storage (G') and loss (G'') modulus were obtained after process completion. All of the rheological tests were carried out at least three times, and the report included the averages of those trials.

2.5 Model fitting of dynamic oscillatory measurements

Data that were collected from frequency sweep analysis of control and quinoa substituted dough samples were displayed as frequency (ω) *versus* G' or G'' in a log–log graph, similar to that described by Ghoshal and Negi.[5] The frequency dispersions of the dynamic mechanical spectra (G' and G'') are essentially straight lines with various slopes and the power law offers a good description of the rheological behaviour of dough inside the LVR. That is why, eqn (1) and (2) were used to fit frequency sweep data as indicated previously by ref. 9.

$$G' = G'_{\omega_1} \times \omega^a \quad (1)$$

$$G'' = G''_{\omega_2} \times \omega^b \quad (2)$$

where G'_{ω_1} (Pa) and G''_{ω_2} (Pa) represent the coefficients of storage and loss moduli, respectively, extrapolated to the initial measuring frequencies ω_1 and ω_2. The parameters a and b denote the dimensionless power law indexes for the storage and loss moduli, respectively.

The overarching term for non-isothermal kinetics that integrates the elastic modulus and reaction rate, the Arrhenius equation and the time–temperature profile is delineated in the subsequent eqn (3).

$$\int_{G'_0}^{G'} \frac{dG'}{G'_n} = k_0 \int_t^0 \exp\left(\frac{-E_a}{RT}\right) dt \quad (3)$$

G'_0 represents the elastic modulus at time 0 whereas G' denotes the value for elastic modulus at time t. E_a denotes the activation energy, k_0 represents the frequency factor, R is the universal gas constant (8.314 J mol^{-1} K^{-1}) and T signifies the absolute temperature (°C). The relationship for the non-isothermal kinetic parameter, derived from experimental data, was established by regression analysis for a system with a linearly increasing temperature. The nth-order equation may be expressed using eqn (4).

$$\frac{dG'}{dt} = kG''^n \quad (4)$$

where k represents the reaction rate constant and n represents the reaction order.

Arrhenius eqn (5) adequately represents the temperature dependency of the reaction rate constant.[10]

$$k = k_0 \exp\left(-\frac{E_a}{RT}\right) \quad (5)$$

Integrating the combination of eqn (4) and (5) produces eqn (6):

$$\ln\left(\pm \frac{dG'}{G''^n dt}\right) = \ln k_0 - \left(\frac{E_a}{RT}\right) \quad (6)$$

Arrhenius-type plots of eqn (6) determined the kinetic parameters E_a and k_0.

2.6 X-ray diffractometry (XRD)

A PANalytical X'Pert PRO diffractometer (Almelo, The Netherlands) was used to do the recrystallization study on dough samples. The apparatus was outfitted with Cu-Kα radiation at a wavelength of 0.15406 Å, working at a current of 30 mA and a voltage of 40 kV. A scan rate of 5° (2θ)/min with a step size of 0.04° (2θ) were used to acquire diffractograms.[11] The total area scanned and the area of the crystalline peak were calculated using Origin Pro software (Origin-Lab Inc., Northampton, MA, USA). Then, the percentage relative crystallinity (RC) of the samples was calculated similar to that reported by Garg *et al.*[12] using eqn (7).

$$\text{RC (\%)} = (\text{area under crystalline peaks})/(\text{total area}) \times 100 \quad (7)$$

2.7 Fourier transform infrared (FTIR) spectroscopy

FTIR absorption spectra of dough samples were recorded using a FTIR spectrophotometer (PerkinElmer Spectrum, USA) over a range of 400–4000 cm^{-1} at a resolution of 4 cm^{-1} using the potassium bromide pellet technique at room temperature. Around 5 mg of finely grounded sample was mixed with 100 mg of dry potassium bromide and an 8 mm pellet was formed under high pressure, which was then mounted in the instrument beam for analysis. Obtained spectra were derived from an average of 32 scans and the data were presented as mean values. Also, the second derivative of the FTIR spectra *i.e.* deconvolution was used as a peak sharpening method to identify the hidden peaks in the characteristic regions of lipid, protein and starch. The FTIR spectrum was deconvoluted with Gaussian curves using the "Multiple Peak fit" tool and Levenberg–Marquardt algorithm featured in the origin software according to the second derivative peak identification after removing the baseline. To estimate the proportion of main bands (lipid, amide I, and starch area) in the dough samples, $R^2 > 0.99$ and $\chi^2 < 0.001$ were the parameters considered while performing the deconvolution as described by Xing *et al.*[13]

2.8 Scanning electron microscopy (SEM)

A JSM 6100 scanning electron microscope (JEOL, Hitachi, Japan) was used to analyse freeze-dried powdered dough samples. To obtain dough samples in powder form, they were frozen at −40 °C (ColdLab, CL model 120–40, Brazil) and subjected to lyophilisation at −59 °C for 24 h (ScanVac Cool Safe, Denmark), which were then sputter coated with gold at an acceleration voltage of 10 kV.[14] SEM pictures acquired at the same magnification (×3.5k) were analysed using the image processing software (ImageJ 1.53j, 2020).

2.9 Differential scanning calorimetry (DSC)

Around 5 mg of powdered dough sample was placed into aluminium pans and sealed securely. The pans were then heated in the calorimeter (DSC, Q20, TA Instruments, USA) utilizing a temperature profile that was comparable to what was recorded in the middle of the crumb when it was baking. DSC scan conditions were set as follows: stabilization of sample at 30 °C for 2 min, then heated to 200 °C at a rate of 10 °C min^{-1}, maintained at 200 °C for 5 min, and finally cooled to 30 °C. The variables associated with the gelatinisation process *i.e.* onset (T_O), peak (T_P), and final (T_F) temperatures, as well as enthalpy value (ΔH_G) of dough samples were derived from the transition curve. To determine amylopectin retrogradation (ΔH_R) as a function of storage time, dough samples after first scan in DSC, were maintained at a fixed temperature (4 °C) for 24 h and 72 h, similar to that described in ref. 15. Subsequent to the designated storage duration, pans were heated again under analogous conditions in the DSC as previously outlined to ascertain ΔH_G. The enthalpy data obtained from DSC were further analyzed using the Avrami equation for model fitting the enthalpy change associated with retrogradation over time using eqn (8).[16]

$$\theta = \frac{H_\alpha - H_t}{H_\alpha - H_0} = e^{-kt^n} \quad (8)$$

Upon linearization, the equation will be

$$\ln(-\ln\theta) = \ln\left[\frac{H_\alpha - H_0}{H_\alpha - H_t}\right] = \ln(k) + n\ln t \quad (9)$$

where, θ represents the proportion of non-retrograded material that remains after time t, k represents the rate constant reflective of the rate of retrogradation, H_0 stands for the enthalpy of the fresh sample, H_t represents the enthalpy change (J g^{-1}) of the retrograded sample after time t, H_α stands for the enthalpy change of the retrograded sample after 72 h, t depicts the storage time in hours and n denotes the Avrami exponent.

2.10 Crumb features and sensory analysis of bread

Three slices were chosen at random and the individual air cells were measured from the centre of the bread loaf that consisted of an area of 80 × 80 mm, using ImageJ software (National Institute of Health, Bethesda, MD, USA). Images were first converted to 8 bit format and the threshold was set manually for each image. Then images were subjected to the binary watershed method and crumb features such as total number of cells, number of cells smaller than 4 mm^2 and mean cell area were determined.[17] The sensory analysis was conducted on the same day as baking in a laboratory under ambient temperature conditions using a 9-point hedonic scale. Consumer acceptability was evaluated for the freshly baked breads by a total of 35 consumers (20 women; 15 men) aged between 20 and 35 years old. They were selected among students and staff members from Food Technology Lab of Dr. SSB UICET Department, Panjab University, Chandigarh. Sensory attributes which were evaluated for bread slices were appearance, texture, aftertaste and overall acceptability.

2.11 Statistical analysis

Each dough sample underwent the measurements at least three times. The data were examined using SPSS 16 (SPSS Inc., Chicago, IL, USA) and one-way ANOVA ($p < 0.05$), as well as Duncan's multiple range test. The results were calculated using Microsoft Excel 2019 version 2306 and presented as the mean ± standard deviation.

3. Results and discussion

3.1 Physiochemical properties of flour blends

Table 1 delineates the chemical components of the flour combinations used in this investigation for bread production. Increasing the amount of QF enhanced the protein, dietary fibre, fat, and ash levels in the flour mixture while reducing its carbohydrate content and hence, suggesting the high nutritional value of QF in comparison to other commonly used gluten-free flour types *i.e.* rice and maize flour.[18] This indicated the ability of utilizing QF to develop health-promoting gluten-free products, similar to that obtained previously by Xing *et al.*[13] with the inclusion of QF at different levels in wheat-based pan bread. Also, levels of carbohydrate content, particularly starch and fiber content, also have an effect on the absorption capacities of flours in food systems, as these are desirable qualities that improve food productivity, consistency, and impart body to the food.[19] From the analysis, it was observed that the Q60 flour sample showed the highest values for WAC and OAC as compared to the control dough. A similar rise was also observed in WAC and OAC of flour blends with the supplementation of 50% of QF in breakfast cereals made from maize flour.[20] Differences in the absorption capacities of flour mixtures might be affected due to the variation in protein content. Other variables, such as varietal distinctiveness, botanical origin or geographical region and harvesting time are known to alter the absorption abilities of flour blends as well.[19,21]

3.2 Oscillatory dynamic rheology of dough samples

3.2.1 Amplitude sweep analysis. An amplitude sweep test was performed on control dough at different frequencies of 0.1, 1.0 and 10 Hz to determine the LVR, which was further used in frequency sweep analysis. Fig. 1(A) illustrates that dynamic measurements, namely G' and G'', exhibited relative independence at strain amplitude (γ) values ranging between 0.001 to slightly above 1, afterwards the values declined. Yazar *et al.*[1] also reported LVR in the range between 0.01% and 1% for different types of gluten-free dough samples. Based on these findings, the linear viscoelastic behaviour was found to be in the region of $10^{-3} \leq \gamma \leq 1$, characterized by a predominant solid-state behaviour ($G' > G''$), followed by a decline in both moduli. Bozdogan *et al.*[20] observed LVR in the range of $10^{-2} \leq \gamma \leq 1$, in the case of quinoa-based gluten free cake batters at a frequency of 10 rad per s. The significant predominance of G' over G'' plainly indicates that gluten-free dough is highly structured and exhibits viscoelastic behaviour, with elastic characteristics (G') markedly surpassing viscous characteristics (G''). However,

Table 1 Characterisation of gluten free bread dough and bread samples[a]

Physiochemical properties	Control	Q40	Q50	Q60
Dough samples				
Moisture	11.25 ± 0.02^{c}	11.30 ± 0.04^{b}	11.31 ± 0.01^{b}	11.36 ± 0.02^{a}
Protein	6.81 ± 0.08^{d}	8.32 ± 0.14^{c}	9.75 ± 0.21^{a}	10.64 ± 0.25^{a}
Dietary fibre	7.44 ± 0.07^{d}	8.89 ± 0.24^{c}	12.67 ± 0.23^{b}	14.53 ± 0.11^{a}
Ash	1.02 ± 0.02^{d}	2.14 ± 0.04^{c}	3.33 ± 0.03^{b}	3.86 ± 0.05^{a}
Fat	2.51 ± 0.04^{d}	3.64 ± 0.15^{c}	4.21 ± 0.12^{b}	5.01 ± 0.10^{a}
Carbohydrates	74.54 ± 0.13^{a}	69.21 ± 0.41^{b}	65.72 ± 0.17^{c}	62.68 ± 0.22^{d}
WAC (g g^{-1})	4.45 ± 0.01^{c}	4.66 ± 0.05^{b}	4.89 ± 0.03^{a}	4.98 ± 0.12^{a}
OAC (g g^{-1})	1.38 ± 0.02^{c}	1.40 ± 0.14^{b}	1.41 ± 0.01^{b}	1.43 ± 0.03^{a}
RC (%)	23.28 ± 0.14^{c}	23.54 ± 0.15^{c}	31.50 ± 0.22^{b}	34.68 ± 0.24^{a}
DO (1047/1022)	1.06 ± 0.01^{b}	1.08 ± 0.01^{b}	1.07 ± 0.02^{b}	1.25 ± 0.03^{a}
DD (995/1022)	1.06 ± 0.02^{c}	1.12 ± 0.01^{b}	1.12 ± 0.02^{b}	1.38 ± 0.03^{a}
Bread samples				
Loaf height (cm)	3.51 ± 0.21^{c}	4.13 ± 0.32^{b}	4.15 ± 0.11^{b}	4.32 ± 0.32^{a}
Specific volume (ml g^{-1})	1.98 ± 0.04^{c}	2.13 ± 0.02^{b}	2.14 ± 0.02^{b}	2.16 ± 0.03^{a}
No. of cells	1066 ± 21^{d}	1101 ± 42^{c}	1353 ± 25^{a}	1238 ± 33^{b}
% area	5.35 ± 0.44^{c}	9.74 ± 0.27^{b}	10.21 ± 0.31^{b}	11.74 ± 0.53^{a}
Appearance	6.54 ± 1.35^{c}	8.02 ± 1.22^{a}	8.05 ± 0.35^{a}	7.53 ± 1.18^{b}
Aftertaste	7.22 ± 0.23^{b}	6.01 ± 0.15^{c}	7.56 ± 0.60^{b}	8.41 ± 0.35^{a}
Texture	6.51 ± 0.31^{b}	8.13 ± 0.14^{a}	8.25 ± 0.31^{a}	8.64 ± 0.23^{a}
Overall acceptability	6.19 ± 0.11^{c}	8.12 ± 0.25^{a}	7.67 ± 0.14^{b}	7.28 ± 0.36^{b}

[a] Values are mean of three replications ± SD. Relevant differences in values are denoted by different alphabets in the same row ($p < 0.05$). Control: rice and maize flour in 50 : 50 ratio; Q40: 40% substitution with quinoa flour; Q50: 50% substitution with quinoa flour; Q60: 60% substitution with quinoa flour; WAC: water absorption capacity; OAC: oil absorption capacity; RC: relative crystallinity; DO: degree of order and DD: degree of double helix.

values for both storage and loss moduli decreased as the frequency increased from 0.1 Hz to 10 Hz. Results obtained were found to be similar with those reported by Sosa *et al.*,[22] as they observed the stress sweep tests at 1 Hz and determined the LVR in the range of $1 \leq \gamma \leq 10^{3}$, with the addition of QF in gluten-free pasta.

3.2.2 Frequency sweep analysis. Fig. 1(B and C) displays the frequency sweep graphs for the control dough as well as the dough samples that include quinoa. In order to assure a linear viscoelastic response, frequency sweep experiments were conducted at a constant strain of 0.5% based on the results of the amplitude sweep analysis (Section 3.2.1). The results indicated that all gluten-free dough samples demonstrated higher values of G' than G'' across the entire frequency range (0.1–100 Hz), which indicated that the dough samples possessed a weak gel characteristic or might show structural resemblance with solids.[16] On the basis of frequency scans, it was observed that all gluten-free dough samples had elevated levels of G' and G'' at higher frequencies than at lower frequencies. This suggested that the incomplete elastic network was the reason why the stressed dough network recovered slowly. Furthermore, the amount of QF included in the formulation had a significant impact on the values of dynamic moduli. In addition, values of the dynamic moduli were highly influenced by the amount of QF in the formulation. The dough samples showed a rise in G' and G'' as a result of the increasing substitution level of QF in the dough mix, which was comparable to the findings reported previously by Bozdogan *et al.*[5] This might be due to the higher levels of protein in QF in comparison to rice and maize flour which resulted in dough reinforcement that might have been the responsible factor for increased values of viscoelastic modules.[2] Zhang *et al.*[9] also observed similar behaviour with increasing levels of QF in wheat dough. They further stated the reason could be due to the smaller starch particles of QF in comparison to rice and maize flour, which led to increased shear resistance in dough mix and thus sensitivity to frequency decreased. An increasing dynamic modulus value with frequency in dough systems suggests improved dough strength and resilience, which is crucial for proper gas cell formation and expansion during baking. A stiffer dough with a higher modulus is less prone to collapse or distortion, which can be beneficial during processing and storage, particularly in the case of gluten-free doughs.

3.2.3 Power law modelling of frequency sweep. For the purpose of fitting the experimental frequency sweep data, a power law model was utilized. The values of the overall G' and G'' at each particular frequency are determined by mathematical equations (*i.e.* $G' = G'_{\omega_1} \times \omega^{a}$ and $G'' = G''_{\omega_2} \times \omega^{b}$, respectively) derived from the power law. Based on the oscillation theory, these equations display the dynamic modulus coefficient (denoted by G'_{ω_1} and G''_{ω_2}), while G' and G'' are the storage and loss modulus, respectively, and exponents a and b represent the slope of the linear part of the curve. It is suitable to consider each of the exponents as the coordination number that measures the structure's rheological behaviour.[9] When the raw data were processed logarithmically, the constants were derived from the linear regression analysis. At every QF substitution level in the dough samples, G' consistently exceeded G''. In

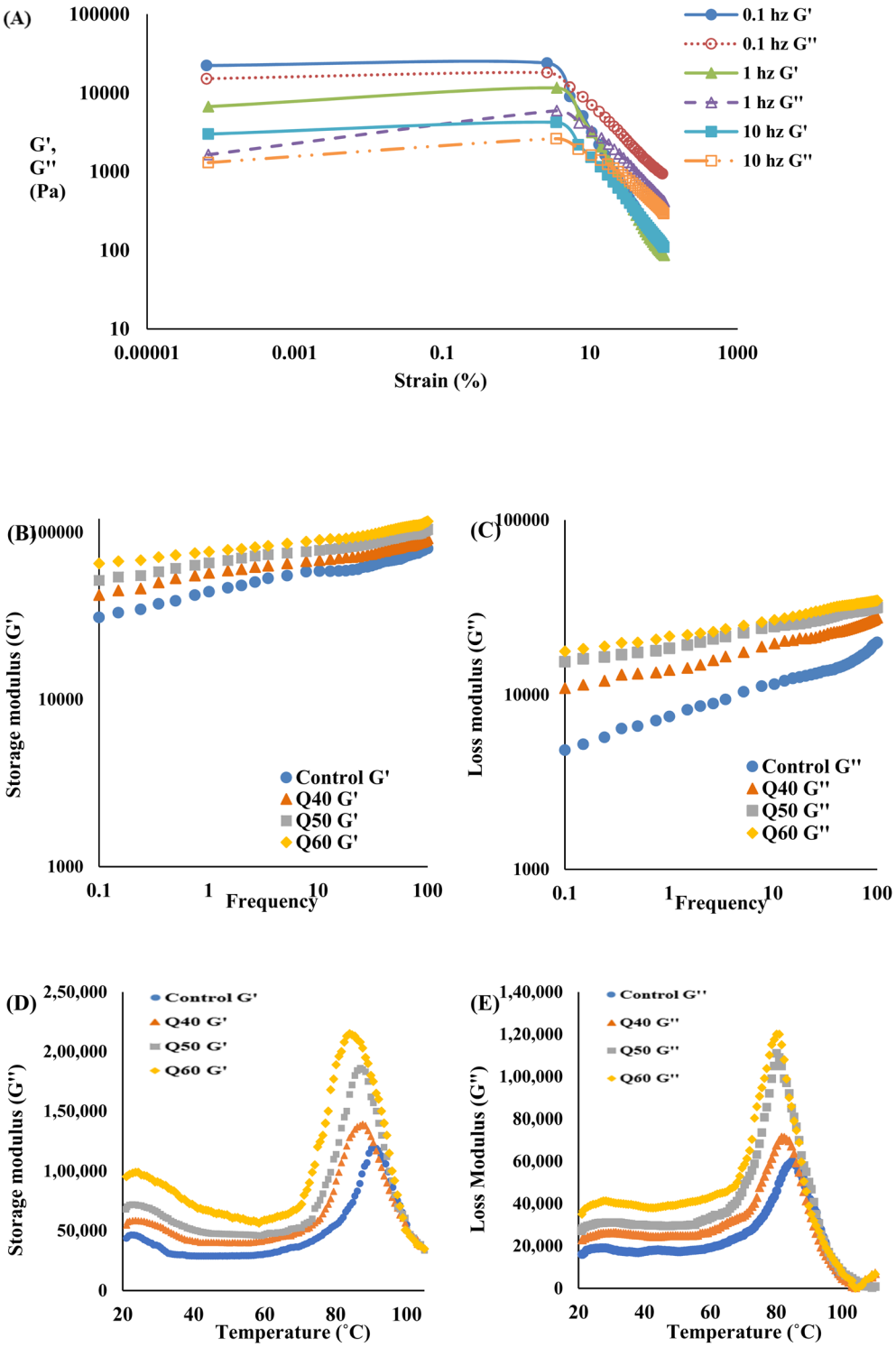

Fig. 1 Dynamic rheology of dough samples. (A) Amplitude sweep curves of control bread dough at different frequencies; (B) storage modulus *vs.* frequency; (C) loss modulus *vs.* frequency; (D) temperature sweep of storage modulus; (E) temperature sweep of loss modulus. Control: rice and maize flour in 50 : 50 ratio; Q40: 40% substitution with quinoa flour; Q50: 50% substitution with quinoa flour; Q60: 60% substitution with quinoa flour.

a similar manner, the values of G'_{ω_1} exceeded those of G''_{ω_2} across all QF substitution levels. The control dough exhibited the lowest values of G'_{ω_1} and G''_{ω_2}, *i.e.* 4.629 Pa and 3.870 Pa, which was followed by the Q40 sample with values of 4.737 Pa and 4.152 Pa, and the Q50 sample, which recorded 4.806 Pa and 4.276 Pa, respectively. However, the Q60 dough sample showed the highest values of G'_{ω_1} and G''_{ω_2} *i.e.* 4.880 Pa and 4.333 Pa, respectively, and hence showed higher dependency on strain.[23]

Exponent a and b values decreased from 0.126 and 0.189 in control dough to 0.099 and 0.133 in Q40, followed by 0.095 and 0.109 in Q50, and 0.081 and 0.102 in the Q60 dough sample, respectively. Thus, values of G'_{ω_1} and G''_{ω_2} increased whereas a and b components decreased as the QF substitution level in dough formulation increased, similar to that reported previously by Ghoshal and Negi.[5] Fig. 2(A–D) represent the frequency sweep model fitting of control and QF substituted dough samples. All four graphs demonstrated a strong fit for both G' and G'', as evidenced by the high R^2 coefficient values ranging from 0.97 to 0.99 (Table 1). G' exceeded G'' in every frequency sweep modelling graph, indicating a predominance of elastic characteristics. The R^2 value was observed to be the highest in the Q50 dough sample for both G' and G'' modulus. The analysis of these graphs led to an understanding that Q50 dough exhibited the best fit within power law equations.

3.2.4 Temperature sweep analysis. The study examined the viscoelastic characteristics at temperatures ranging from 20 °C

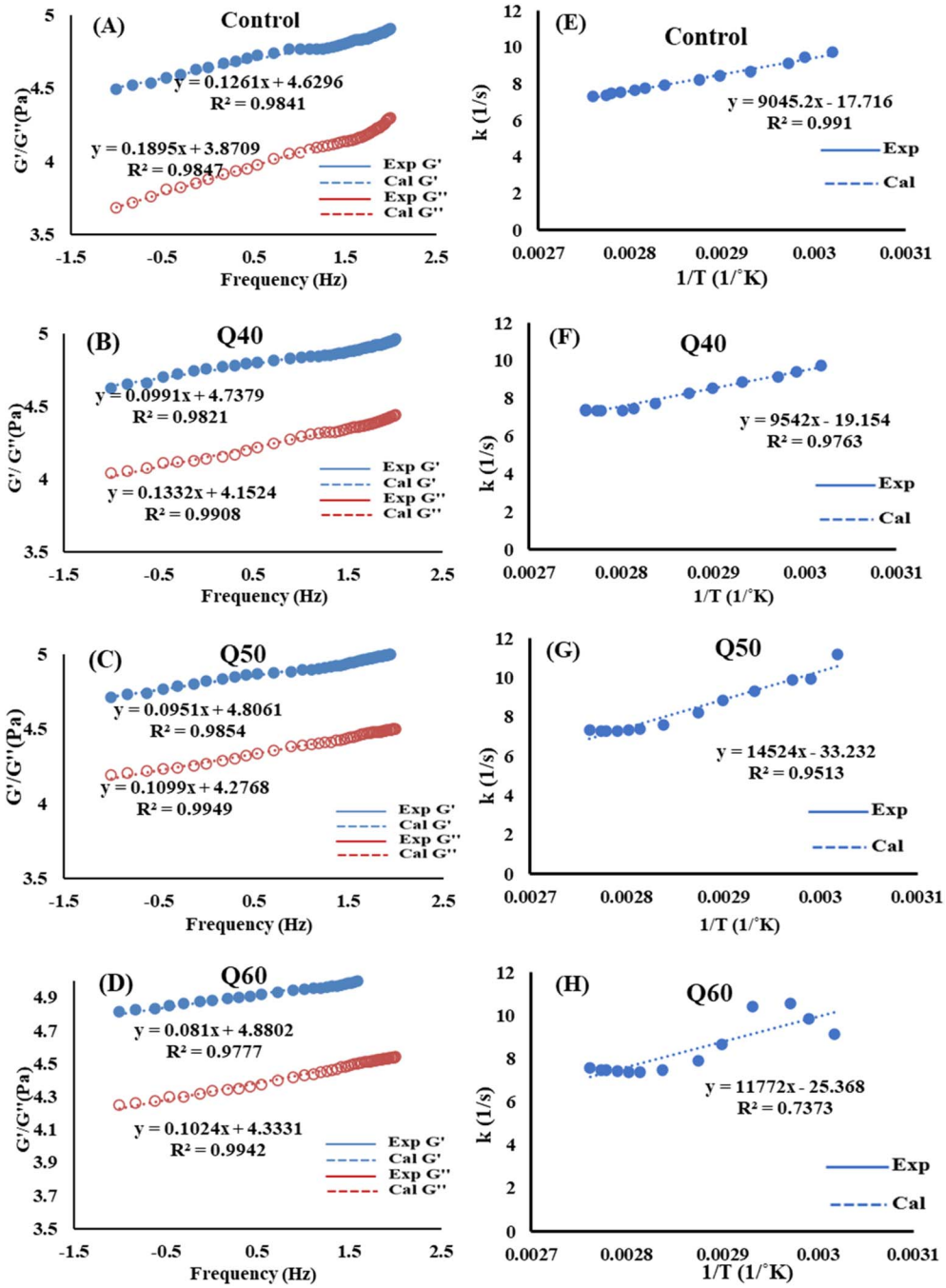

Fig. 2 (A–D) Power law modelling of gluten free dough samples. (E–H) Arrhenius plot of the upward gelatinisation curve of dough samples (first order kinetics). Control: rice and maize flour in 50 : 50 ratio; Q40: 40% substitution with quinoa flour; Q50: 50% substitution with quinoa flour; Q60: 60% substitution with quinoa flour.

to 100 °C. The temperature sweep curves for the dough samples are shown in Fig. 1(D and E). The results indicated that the QF level had a considerable effect on G' and G'' across the whole temperature range. During the temperature sweep test, three separate phases of transition were identified in G' and G''. During the initial phase, both G' and G'' exhibited a decline when the temperature escalated from 20 °C to 60 °C, attributed to the thermal stimulation or energy absorbed by the starch molecules, similar to that reported by Bozdogan *et al.*[5] with the addition of QF in gluten-free cake batter. G' and G'' slightly decreased during the early heating phases as the starch granules started to explode and release the water they had absorbed, causing the starch to gelatinize eventually. Because of the denaturation of proteins and the swelling of starch molecules that were present, structure development began as soon as the temperature reached a level that was higher than the critical temperature (temperature at which G' and G'' attain their lowest possible values). At this phase, gelatinization of the starch speeded up considerably and both G' and G'' started to increase rapidly. In addition, the temperature at which the control dough underwent gelatinization was much higher than quinoa containing dough samples. This suggests that the control dough required a greater amount of thermal energy in order to be completely gelatinized. In the last phase, G' and G'' began to decline after attaining peak at a certain temperature, due to the culmination of structural alterations. The observed decline in all gluten-free dough samples indicated that the higher amount of proteins in quinoa containing dough samples contributed to greater resistance of starch granules to disintegration. Consequently, the denatured proteins reinforce the continuous dough network and contribute to the mechanical strength of the dough samples throughout the baking process.[24] The two moduli exhibited analogous fluctuations with temperature and G'' consistently lower than G' across all temperatures, suggesting that the starch gel demonstrated higher degree of elasticity than viscosity.

3.2.5 Non isothermal heating pattern of dough. Fig. 2(E–H) show the gluten-free dough samples' non-isothermal heating trend. The dynamic modulus increased dramatically with treatment temperature, reached its highest point and then fell progressively until levelling out. The gelatinization process was represented by the curve that was situated beneath the peak, which was analogous to the DSC derived curve. Two primary segments were responsible for the gelatinization process: the upward curve and the descending curve. The first half of the curve depicted the pre-gelatinization phase, which was characterized by the partial swelling of the starch granules in an aqueous medium, while the second half presented the gelatinisation step where the amylose component breaks down and leaches out. It was anticipated that the reaction kinetics for these two segments would vary from one another. The temperature range that was used for the kinetic analysis in this experiment was from 50 °C to 90 °C. This temperature range was chosen since it was deemed to be the temperature at which G' and G'' reached their highest possible value. In order to investigate the kinetics of the dough starch gelatinization reaction, non-isothermal heating was used. This is due to the fact that the heating of starch dough in an isothermal manner is influenced by both the temperature and the time of the heating process.[10] It is generally agreed that the non-isothermal methodology is the most effective method among the numerous kinetic models. This is due to the fact that the majority of gelatinization kinetics experiments have been conducted *in situ* at a constant heating rate, and the change in G' quantifies the structure development rate (dG'/dt).[25] All the gluten-free dough composites had their activation energies (E_a) estimated using an Arrhenius-type relationship. The Runge–Kutta fourth order reaction kinetics were employed to solve eqn (3) for a nonlinear ordinary differential equation. The findings from the experimental plot of G' *vs.* temperature can be used to evaluate k_0, reaction order and E_a. Kinetic parameters were calculated using first and second order reactions as shown in Table 2S. It became apparent that the first order reaction resulted in the best fit for the rising curve, also known as pre-gelatinized kinetics.

3.3 Crystallinity of dough samples

Fig. 3(A) displays the XRD diffractograms of all the dough samples that were freeze-dried. The characteristic X-ray patterns in all dough composites indicated that the starch crystal structure reflected to the A-type polymorph of amylopectin, which happens to be characteristic of cereal starches. This polymorph is characterized by significant reflections at 15°, 20°, and 23° (2θ), as well as an unresolved doublet at 2 values of 17° and 18°, which is comparable to what was observed by Azizi *et al.*[3] The existence of the starch–lipid complex resulted in the appearance of a tiny absorption peak at a 2θ value of 20°, which was V-shaped. There was a correlation between the crystalline form at 20° (2θ) and the interaction between amylose and amylopectin in the starch.[26] On comparing the XRD diffractograms, it was observed that with the incorporation of QF did not change the A-type pattern, but peak intensities at 15°, 17° and 18° (2θ) increased slightly. This was also evident in the values of relative crystallinity (RC) as it increased from 23.28% for control dough to 23.54%, 31.50% and 34.68% for Q40, Q50 and Q60 dough samples, respectively (Table 1). This variance may be the result of a number of aspects, such as differences in the ratio of amylose to amylopectin, the structure of the starch, and interactions between the starches or with other ingredients in the blend that may have an effect on the WAC of the various other starches that are involved. Introducing QF might facilitate more interactions between amylopectin and amylose chains that resulted in the rearrangement and perfection of crystalline regions of starch granules. Additionally, there was a negative relationship between the amount of amylose and the crystallinity of the dough samples. According to earlier research, the starch in QF has a low amylose percentage (with values varying from 5.6% to 11.0%) in comparison to the majority of cereal starches.[12] This indicated that the addition of QF effectively diluted the overall amylose percentage in the final dough mixture, which further explained the reduction in the intensity of the peak at 20° (2θ) in the X-ray diffraction (XRD) pattern.[27] Ma *et al.*[28] also observed dilution of the overall amylose content

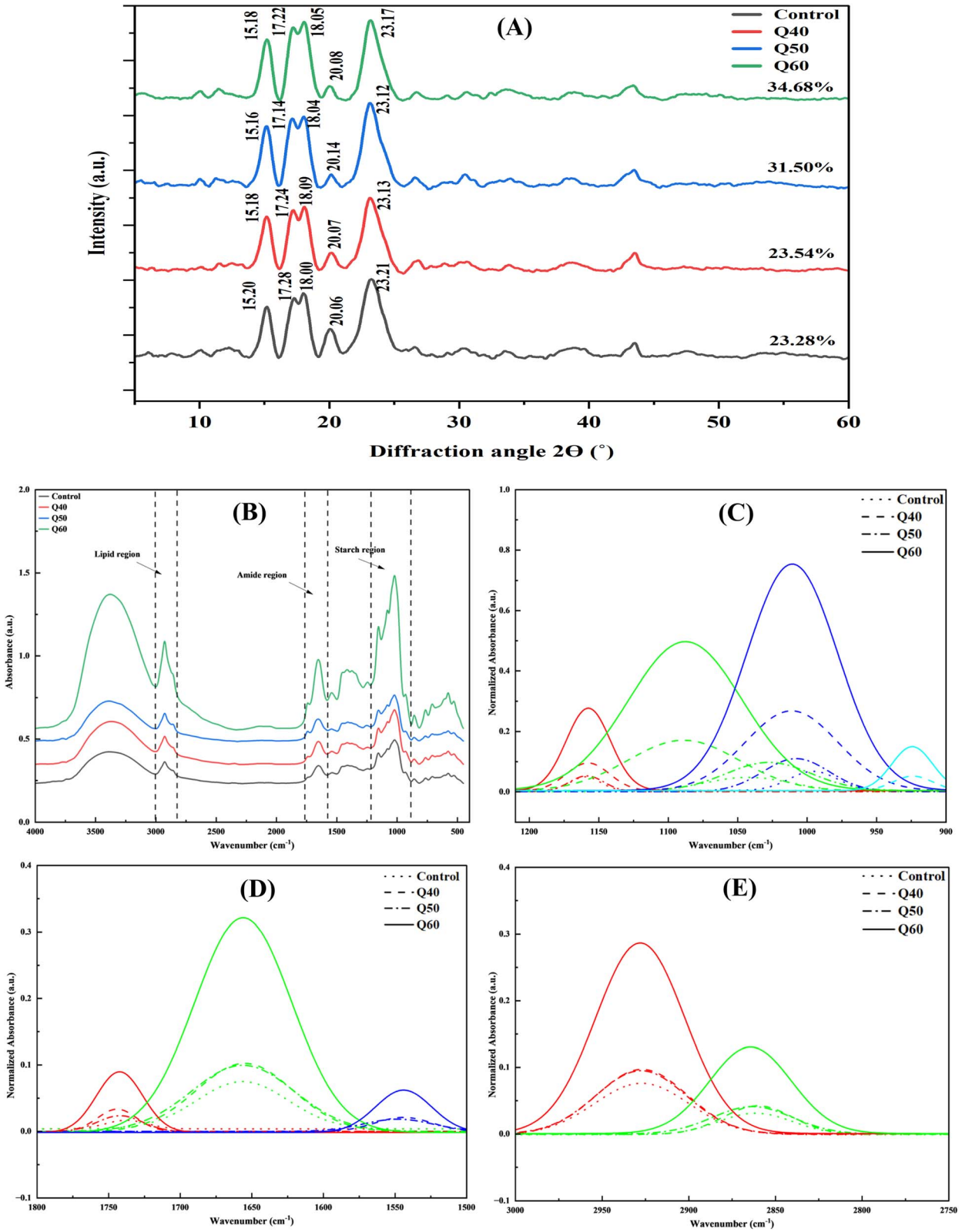

Fig. 3 (A) XRD plots of gluten free bread dough samples. (B) Absorption spectra of gluten free dough samples. Control dough: black line (—), Q40 dough: red line: (—), Q50 dough: blue line (—), Q60 dough: green line (—); (C) deconvolution spectra of starch region; (D) deconvolution spectra of amide region; (E) deconvolution spectra of lipid region. Control dough: dotted line (···); Q40 dough: dash dot line (–·–·); Q50 dough: dash dash line (– – –); Q60 dough: solid line (—).

with increasing QF addition levels in wheat-based dough samples.

3.4 FTIR spectra of dough samples

In this work, the structural composition of gluten-free dough samples was analysed by the FTIR analytical technique. The positions of characteristic peaks in the FTIR spectrum at around 3387, 2922, 1653, 1150 and 1080 cm^{-1} for all dough samples did not vary significantly, indicating that no new functional group formation occurred with quinoa addition (Fig. 3(B)). FTIR absorbance ratios at 995/1022 cm^{-1} and 1047/1022 cm^{-1} increased noticeably (Table 1), indicating a rise in the proportion of double helices and short-range molecular order.[12] The results are in close concordance with the percentage RC values obtained from XRD (Section 3.3). The FTIR spectra were further deconvoluted from 900–1200 cm^{-1}, 1500–1800 cm^{-1} and 2750–3000 which represented starch, amide and lipid regions, respectively, for all dough samples as displayed in Fig. 3(C–E). Two glycosidic bands at 1080 and 1150 cm^{-1} associated with the amylaceous content were observed due to the vibrations of the C–O–C functional group.[29] The presence of a noteworthy peak at 1653 cm^{-1} could possibly be related to the stretching of the C═O bonds in the amide I groups, in conjunction with the bending of the O–H bonds in water (Fig. 3(D)). An additional peak that is associated with proteins became apparent at a frequency of 1545 cm^{-1} (the amide II band). This peak was associated with C–N and C–C stretching as well as N–H bending that takes place in gluten proteins.[13] The intensity of the amide I peak was significantly greater than the amide II peak in all the dough samples, similar to that reported earlier for different quinoa coproducts obtained by the wet milling process by Ortiz-Gómez *et al.*[30] Consequently, only the amide I band area (1700–1600 cm^{-1}) may be utilized to define the secondary structure of proteins, owing to its greater susceptibility to protein conformation in comparison to amide II. Fig. 3(E) illustrates the intensities within the range of 2800 to 3000 cm^{-1}, indicative of lipids. The bands at 2922 cm^{-1} and 2854 cm^{-1} are associated with the symmetric and asymmetric stretching of CH_2 aliphatic groups, respectively, while the band observed at 1745 cm^{-1} was related to the stretching of the ester carbonyl group.[31] It was found that elevating QF in dough formulation resulted in increased intensity of peaks in starch, protein and lipid regions due to increased vibrations and conformational changes in functional group C–O–C, NH_2 and lipid acyl chains, respectively. Several researchers recently identified a similar association between different components of flour (*i.e.* starch, protein, and lipids) and their respective band intensities (1150 cm^{-1}, 1648 cm^{-1}, and 2925 cm^{-1}), therefore establishing a relationship between them.[29,30]

3.5 Morphology of dough samples

Dough samples display uniform homogeneous structures. This configuration can be referred to the arrangement of starch molecules during dough development caused by shear stress, as well as the generation of a cross-linked network by proteins in the dough using covalent, hydrogen, hydrophobic, and ionic interactions.[14] Fig. 4(A–D) show the scanning electron micrographs (SEM) of freeze-dried dough samples. Images captured the shape of starch granules with other flour constituents, including fiber, protein complexes, and additives. The average particle size of the freeze-dried dough samples declined as the proportion of QF in the gluten-free dough formulation increased. This might be because the quinoa granules were smaller than the other flours in the dough.[18] The smallest particle exhibiting significant size variability was identified in quinoa starch granules, with measurements ranging from 0.59 μm to 3.41 μm. The differences in granule shape among the three distinct starches in the dough formulation may be attributed to their biological origin and changes in the amylopectin and amylose levels. Also, the particles of QF exhibited irregular shapes and were observable both singly and in aggregate, which is characteristic of mostly small-sized starch granules.[12] The diminutive size and morphology of quinoa starch granules offer distinctive processing benefits, including greater resilience under high shear conditions, capacity to serve as carrier molecules for colorants and flavor compounds, and application as fat substitutes. These may further influence the physicochemical qualities, pasting characteristics, and digestibility of gluten-free bread.[32,33]

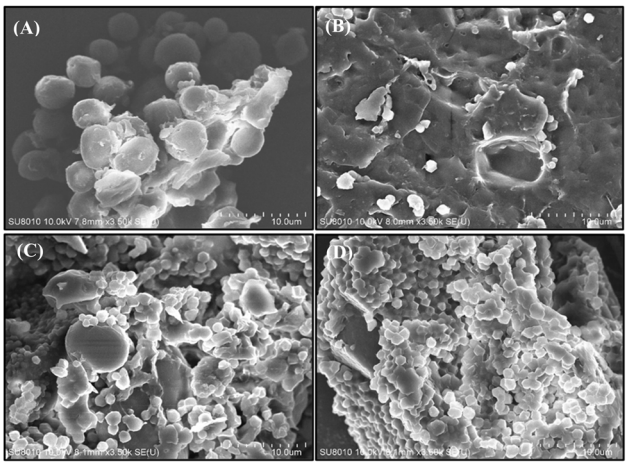

Fig. 4 SEM images of gluten free bread dough samples at ×3.5k magnification. (A) Control sample; (B) Q40 sample (40% substitution with quinoa flour); (C) Q50 sample (50% substitution with quinoa flour); (D) Q60 sample (60% substitution with quinoa flour).

3.6 Thermal properties of dough samples

Thermogravimetric analysis of freeze-dried dough samples provided the thermal parameters listed in Table 2, with the corresponding thermograms displayed in Fig. 5(A). Within the temperature range of 40 °C to 200 °C, each of the dough formulation showed one endothermic transition. The gelatinisation conditions of dough during the baking process were attempted to be replicated by selecting this temperature range. A prominent endothermic peak with an extended tail appeared in the first scan, which correlated with the gelatinisation profile of the dough samples. The water level was sufficiently high to

Table 2 DSC parameters, Avrami exponents and time constants of gluten free bread dough samples[a]

	Gelatinisation of dough samples			
Samples	Control	Q40	Q50	Q60
T_O (°C)	44.65 ± 0.03[a]	44.26 ± 0.11[a]	43.18 ± 0.05[b]	44.27 ± 0.01[a]
T_P (°C)	83.05 ± 0.17[c]	83.09 ± 0.02[c]	84.24 ± 0.64[b]	85.13 ± 0.83[a]
T_F (°C)	87.08 ± 0.28[c]	87.37 ± 0.15[c]	88.07 ± 0.78[b]	90.13 ± 0.44[a]
ΔH_G (J g^{-1})	2.88 ± 0.62[a]	2.49 ± 0.02[b]	2.00 ± 0.48[c]	1.85 ± 0.07[d]
Amylopectin retrogradation (J g^{-1}) of DSC scanned dough after 3 day storage at 4 °C				
24 h	3.84 ± 0.41[a]	2.95 ± 0.28[b]	2.46 ± 0.15[c]	2.36 ± 0.77[c]
72 h	5.21 ± 0.06[a]	3.22 ± 0.03[b]	2.94 ± 0.52[b]	2.62 ± 0.38[c]
n	0.95 ± 0.42[b]	0.95 ± 0.42[b]	0.95 ± 0.42[b]	0.95 ± 0.42[b]
k	0.027 ± 0.002[b]	0.013 ± 0.001[c]	0.173 ± 0.005[a]	0.172 ± 0.001[a]
R^2	0.997	0.999	0.985	0.973

[a] Values are mean of three replications ± SD. Relevant differences in values are denoted by different alphabets in the same row ($p < 0.05$). T_O: onset temperature; T_P: peak temperature; T_F: final temperature; ΔH_G: gelatinisation enthalpy.

encourage starch gelatinization, evidenced by the presence of a single endotherm.[15] Elevating the QF level in the dough composite resulted in a significant increase in T_P and T_F, except for T_O which displayed a similar value *i.e.* around 44 °C (Table 2). This might be due to the presence of high protein and fiber content in quinoa containing dough samples that compete with starch for water.[3] The incorporation of quinoa led to a progressive reduction in ΔH_G, similar to that reported previously by Chiotelli and Le Meste.[33] They stated that large sized starch granules require higher gelatinisation enthalpy than the smaller ones. The small size of quinoa starch particles in comparison to the other types of starches present in the dough composites might be the cause of the lower ΔH_G values of dough samples that contain quinoa. Moreover, a negative correlation was identified between the gelation enthalpy *i.e.* ΔH_G assessed using DSC and RC (%) values obtained from XRD analysis (Section 3.3), which was also reported previously by Skendi *et al.*[11]

3.6.1 Retrogradation studies. Amylopectin retrogradation, which is the recrystallization of starch molecules in baked dough, can be monitored using DSC. Samples obtained after the first DSC scan were further stored at 4 °C for 72 h *i.e.* 3 days as most of the starch retrogradation occurred within first three days of storage, after that the effects were only moderate.[3] These also presented single peaks that correlated with the melting of the retrograded amylopectin component in all gluten-free dough composites. The endothermic peak was observed at a temperature that was comparable across all dough samples (around 50 °C), although variations in retrogradation enthalpies *i.e.* ΔH_R were observed. A significant increase ($p < 0.05$) in the value of ΔH_R was observed in all dough composites during storage. Nonetheless, ΔH_R strategically decreased from 3.84 J g^{-1} to 2.36 J g^{-1}, after the second scan (24 h of storage) and 5.21 J g^{-1} to 2.62 J g^{-1}, after the third scan (72 h of storage) with increasing levels of QF in the dough mixture (Table 2). This might be due to the presence of shorter amylopectin chains with the inclusion of QF in dough formulation that required less energy to dissociate completely.[12] The observed variations in the DSC parameters across the different dough samples could potentially originate from the interplay between dough hydration levels and the amount of QF utilised in gluten-free bread dough formulation.[34]

3.6.2 Retrogradation kinetics. To investigate the variation of enthalpy with storage in dough samples, crystallization data were modelled using the Avrami equation, and model parameters were determined by fitting experimental data for melting enthalpies to the nonlinear regression eqn (8). The test points of enthalpy values obtained at 0, 2, 24, 48, and 72 h of storage were used to determine Avrami coefficients (n,k). Enthalpy values were computed and plotted using calculated Avrami coefficients (Fig. 5(B)). As shown in Table 2, recrystallization kinetics data were well suited to the Avrami equation since the R^2 values were close to 1 ($R^2 > 0.97$). The Avrami constant, n, is linked to the morphology of crystals and quantifies their growth process.[16] Regression parameters of eqn (8) yield the values of n and k. Values of n firstly increased from 0.955 in control to 1.344 in the Q40 sample, which then decreased to 0.458 and 0.871 for Q50 and Q60 samples, respectively. The value of rate constant (k) varied from 0.027 in control to 0.013 in Q40 and 0.173 in Q50 and Q60 samples. Analysis indicated that the incorporation of QF produced a softer crumb and restricted the rate of staling in DSC scanned dough samples. It confirmed that quinoa addition reduced the crystal growth and rate of staling slightly in DSC scanned dough samples. Reduction of limiting enthalpy (H_α) values was observed from 5.21 J g^{-1} in control dough to 3.22, 2.94 and 2.62 J g^{-1} for Q40, Q50, and Q60 dough samples, respectively (Table 2), similar to that reported previously by Vicente *et al.*[35] Therefore, from the above results, it can be concluded that QF inclusion in bread dough formulation slowed down the crystallization rate and growth of crystals which was directly reflected in enthalpy values. These results also supported the XRD results (Section 3.3).

3.7 Crumb features of bread slices

Elevating quinoa flour levels in gluten free bread formulation increased the total number of gas cells detected in the regions of interest *i.e.* from 1066 ± 21 in control bread, to 1101 ± 1238 ± 33 in the Q60 bread sample (Table 1). However, the percentage

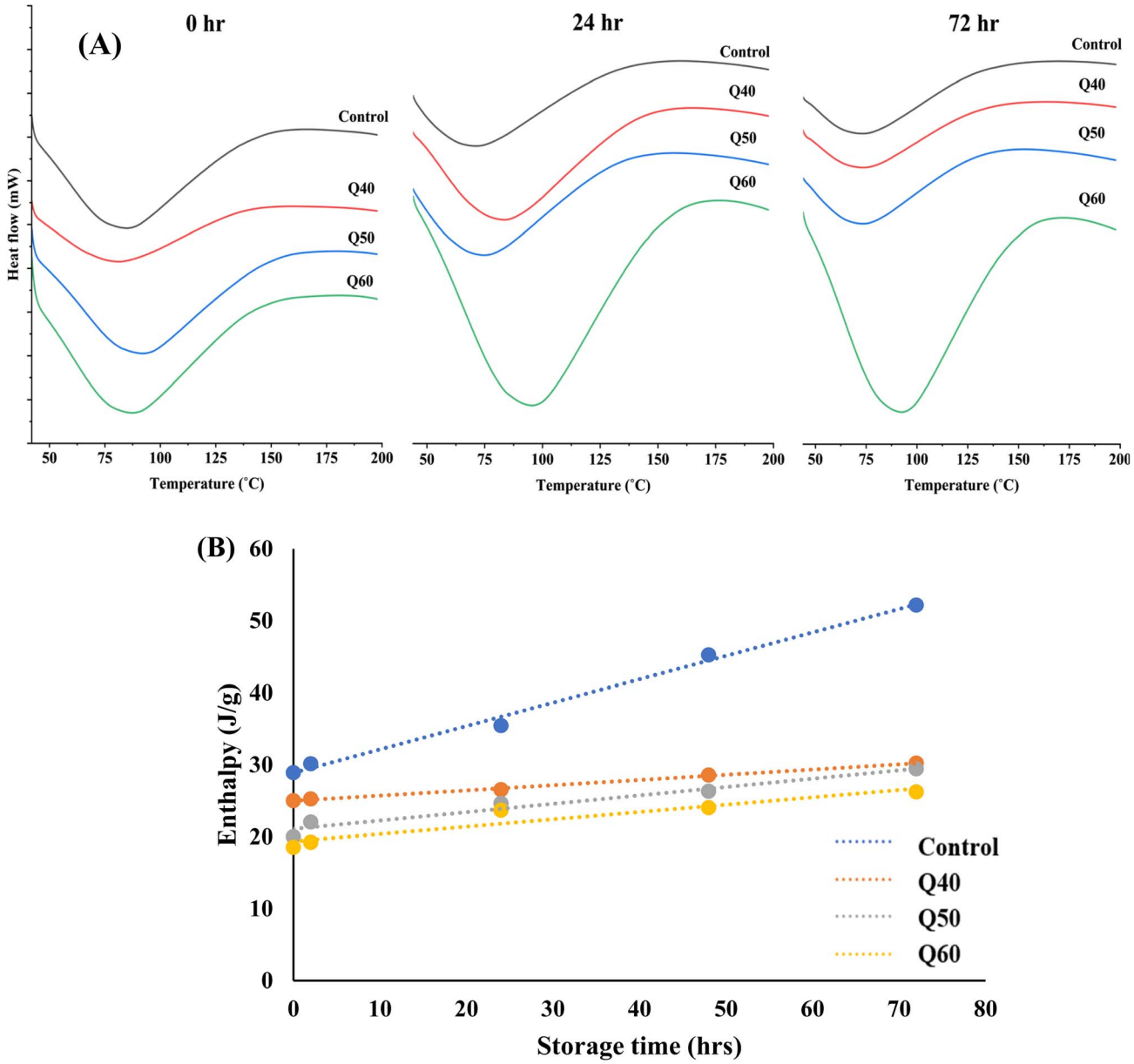

Fig. 5 (A) DSC thermograms of gluten free dough samples; (B) temporal variation of enthalpy values of gluten free dough samples. Control: rice and maize flour in 50 : 50 ratio; Q40: 40% substitution with quinoa flour; Q50: 50% substitution with quinoa flour; Q60: 60% substitution with quinoa flour.

area occupied by gas cells was 5.35% in the case of control bread, which increased to 9.74%, 10.21% and 11.74% for Q40, Q50 and Q60 bread samples, respectively. This suggested that cell density decreased with increasing quinoa flour substitution level in bread formulation. Results obtained were similar to that reported earlier by Azizi *et al.*,[27] as they reported significant increase in pore intensity of gluten free bread when the amount of quinoa flour increased from 15% to 25%. This indicated that the incorporation of quinoa flour improved the gas retention capacity of the dough matrix as cell density decreased and void fraction increased. The higher void fraction indicates a more open structure, which has been related positively to the specific volume of the bread as well as with the gas retention capacity of the dough.[36] Also, breads supplemented with quinoa flour showed a slight reduction in circularity value with values ranging from 0.83 to 0.84 for quinoa substituted samples, as compared to control bread with a cell circularity of 0.89, similar to that reported by Ballester-Sánchez *et al.*[34] and Vicente *et al.*[37] This indicated that the integrity of gas cells and bread crumb uniformity were maintained throughout the course of the breadmaking process as small gas cells did not coalesce into larger ones during breadmaking.

3.8 Baking quality of bread

Control bread achieved the lowest height *i.e.* 3.51 cm as compared to quinoa substituted breads (4.13 cm to 4.32 cm) as

shown in Table 1. Specific volume values of the gluten free bread loaves increased by 7.57%, 8.08% and 9.08% with increasing quinoa flour substitution levels of 40%, 50% and 60%, respectively. This could be related to the higher visco-elasticity of doughs achieved because of higher protein–starch interactions in quinoa containing doughs in comparison to control dough which would help in retaining more gas during baking.[24] Vicente *et al.*[37] and Di Renzo *et al.*[38] also reported improved loaf height and specific volume in quinoa fortified gluten free breads. Mean hedonic ratings of sensory attributes (appearance, taste, and overall acceptability) for all the gluten free breads are presented in Table 1. The data indicated that the mean sensory score of appearance for control bread was 6.54 which represented "like slightly" whereas quinoa containing breads had an appearance score of 8.03, 8.05 and 7.93, for Q40, Q50 and Q60 bread samples, respectively, which represented "like very much" on the sensory scale. According to Turkut *et al.*,[6] gluten free breads prepared mostly from starches or refined flours were usually identified by having lighter color, thus darker color breads were usually preferred and given higher scores. Franco *et al.*[39] also observed intense color values of crust with the addition of germinated quinoa in gluten free bread formulation. Further analysis revealed taste scores were higher in Q40 and Q50 bread samples *i.e.* 8.29 and 8.01, respectively, as compared to control (7.13) and Q60 (6.11) bread sample, which might be related to the slight bitterness perceived in Q60 bread. It is worth mentioning that the addition of quinoa flour in bread up to 50% level *i.e.* Q40 and Q50 bread, gave the bread an exceptional flavour with a nutty taste and no bitterness after tasting, similar to that observed by El-Sohaimy *et al.*[40] with the supplementation of quinoa flour in pan bread.

4. Conclusion

The way dough behaves mechanically affects the steps of processing, including dividing, rounding, and moulding, and it could change depending on the end product's properties. In the present study, QF was incorporated at various proportions in gluten-free composite dough. Increasing G' and G'' values with frequency in dough systems suggest improved strength and resilience, which are crucial for proper gas cell formation and expansion particularly in the case of gluten-free doughs. The power law model was fitted to assess data adequacy. In all four graphs, it was observed that both G' and G'' fitted well as indicated by the higher value of the R^2 coefficient. DSC demonstrated a decrease in enthalpy values with the inclusion of quinoa, which can also be ascribed to the small starch granules present in quinoa. Dough sample analysis revealed considerable negative correlation between gelation enthalpy and crystallinity. Also, introducing QF might facilitate more interactions between amylopectin and amylose chains which resulted in the rearrangement and perfection of crystalline regions of starch granules as indicated by FTIR and XRD analysis. Consequently, fundamental rheological testing methods serve as a potent technique for analysing the microstructural features of substances. Although all quinoa containing bread samples demonstrated acceptable technological properties, slight bitterness was observed during sensory analysis in the Q60 bread sample. These results demonstrate the potential of quinoa flours in formulating healthier gluten-free breads that may further offer essential direction to help improve the production and optimisation of mixed-grain gluten-free breads.

Conflicts of interest

There is no conflict of interest between the authors.

Data availability

All data generated or analyzed during this study are included in this published article.

The supporting data has been provided as part of the supplementary information (SI). Supplementary information: Tables 1S and 2S. See DOI: https://doi.org/10.1039/d5fb00763a.

Acknowledgements

Priyana Garg is thankfull to TEQIP III, Dr S. S. BUICET, Panjab University, Chandigarh for her fellowship.

References

1 G. Yazar, O. Duvarci, S. Tavman and J. L. Kokini, *J. Cereal. Sci.*, 2017, **74**, 28–36.
2 L. Sciarini, M. Steffolani, A. Fernández, C. Paesani and G. Pérez, *Food Sci. Technol. Int.*, 2020, **26**, 321–332.
3 A. I. Gostin, *LWT–Food Sci. Technol.*, 2019, **114**, 108412.
4 A. Cappelli, N. Oliva and E. Cini, *Appl. Sci.*, 2020, **10**, 6559.
5 G. Ghoshal and P. Negi, *Food Bioprod. Process.*, 2020, **124**, 342–353.
6 G. M. Turkut, H. Cakmak, S. Kumcuoglu and S. Tavman, *J. Cereal. Sci.*, 2016, **69**, 174–181.
7 AACC International, *Approved Methods of Analysis*, St. Paul, MN, 11th edn, 2010.
8 AOAC International, in *Official Methods of Analysis*, Gaithersburg, MD, USA, 18th edn, 2006.
9 Y. Zhang, X. Wang and X. Guan, *Int. J. Food Sci. Technol.*, 2022, **57**, 7099–7106.
10 M. Alvarez, F. Cuesta, B. Herranz and W. Canet, *Foods*, 2017, **6**, 3.
11 A. Skendi, M. Papageorgiou and E. Papastergiadis, *J. Food Process. Preserv.*, 2022, **46**(10), e15876.
12 P. Garg, G. Ghoshal, J. Garg and M. Goyal, *Int. J. Biol. Macromol.*, 2025, **303**, 140677.
13 B. Xing, Z. Zhang, M. Zhu, C. Teng, L. Zou, R. Liu, L. Zhang, X. Yang, G. Ren and P. Qin, *Food Chem.*, 2023, **399**, 133976.
14 J. Ding, H. Hu, J. Yang, T. Wu, X. Sun, Y. Fang and Q. Huang, *Innov. Food Sci. Emerg. Technol.*, 2023, **83**, 103217.
15 M. Witczak, R. Ziobro, L. Juszczak and J. Korus, *Food Bioproc. Tech.*, 2021, **14**, 65–77.
16 J. O. Kim, W. S. Kim and M. S. Shin, *Starch/Staerke*, 1997, **49**, 71–75.
17 A. Skendi, P. Mouselemidou, M. Papageorgiou and E. Papastergiadis, *Food Chem.*, 2018, **253**, 119–126.

18 S. O. Abogunrin and O. J. Ujiroghene, *Asian Food Sci. J.*, 2022, 38–51.
19 S. A. Oyeyinka, A. I. Adebayo, A. T. Oyeyinka, A. O. Akeem, T. Garuba and A. O. Oladunjoye, *J. Food Process. Preserv.*, 2021, **23**(12), 2078–2079.
20 N. Bozdogan, S. Kumcuoglu and S. Tavman, *J. Food Sci. Technol.*, 2019, **56**, 683–694.
21 S. A. El-Sohaimy, M. G. Shehata, T. Mehany and M. A. Zeitoun, *Int. J. Food Sci.*, 2019, **2019**, 1–15.
22 M. Sosa, A. Califano and G. Lorenzo, *Eur. Food Res. Technol.*, 2019, **245**, 343–353.
23 S. Mironeasa and G. G. Codină, *Foods*, 2019, **8**, 626.
24 K. Shevkani, A. Kaur, S. Kumar and N. Singh, *LWT–Food Sci. Technol.*, 2015, **63**, 927–933.
25 J. Ahmed, A. S. Almusallam, F. Al-Salman, M. H. AbdulRahman and E. Al-Salem, *LWT–Food Sci. Technol.*, 2013, **51**, 409–416.
26 N. A. Mir, C. S. Riar and S. Singh, *Trends Food Sci. Technol.*, 2018, **75**, 170–180.
27 S. Azizi, M. H. Azizi, R. Moogouei and P. Rajaei, *Food Sci. Nutr.*, 2020, **8**, 2373–2382.
28 Y. Ma, L. Guo, Y. Chen, S. Yan, L. Wang, K. Zhao, H. Li, J. Liu, D. Li, W. Zhang, X. Duan, X. Liu, X. Cao and X. Gao, *LWT–Food Sci. Technol.*, 2025, **223**, 117804.
29 D. F. Roa-Acosta, J. E. Bravo-Gómez, M. A. García-Parra, R. Rodríguez-Herrera and J. F. Solanilla-Duque, *LWT–Food Sci. Technol.*, 2020, **121**, 108952.
30 V. Ortiz-Gómez, A. Fernández-Quintero, D. F. Roa-Acosta, J. E. Bravo-Gómez and J. F. Solanilla-Duque, *Front. Sustain. Food Syst.*, 2022, **6**, 851433.
31 Á. J. García-Salcedo, O. L. Torres-Vargas and H. Ariza-Calderón, *Acta Agron.*, 2017, **67**, 215–222.
32 J. Ruales, S. Valencia and B. Nair, *Starch/Staerke*, 1993, **45**, 13–19.
33 E. Chiotelli and M. Le Meste, *Cereal Chem.*, 2002, **79**, 286–293.
34 J. Ballester-Sánchez, E. Yalcin, M. T. Fernández-Espinar and C. M. Haros, *Eur. Food Res. Technol.*, 2019, **245**, 1571–1582.
35 A. Vicente, M. Villanueva, P. A. Caballero, J. M. Muñoz and F. Ronda, *Foods*, 2023, **12**, 1421.
36 J. J. Burbano, J. P. Di Pierro, C. Camacho, J. Vidaurre-Ruiz, R. Repo-Carrasco-Valencia, F. A. Iglesias, M. Sánchez, Y. A. M. Ospina, D. E. Igartúa, M. J. Correa and D. M. Cabezas, *Plant Foods Hum. Nutr.*, 2025, **80**, 33.
37 A. Vicente, M. Villanueva, P. A. Caballero, A. Lazaridou, C. G. Biliaderis and F. Ronda, *Food Hydrocoll.*, 2024, **155**, 110244.
38 T. Di Renzo, M. C. Trivisonno, S. Nazzaro, A. Reale and M. C. Messia, *Foods*, 2024, **13**, 1382.
39 W. Franco, K. Evert and C. Van Nieuwenhove, *Fermentation*, 2021, **7**, 115.
40 S. El-Sohaimy A., M. Shehata G., T. A. Djapparovec, T. Mehany, M. Zeitoun A. and A. Zeitoun M., *J. Food Process. Preserv.*, 2021, **45**(2), e15180.